IOP Conference Series: Materials Science and Engineering

Dimensional structural mass optimization of forged steel connecting rod for aircraft piston engine

To cite this article: M Helal *et al* 2021 *IOP Conf. Ser.: Mater. Sci. Eng.* **1172** 012001

Dimensional structural mass optimization of forged steel connecting rod for aircraft piston engine

M Helal[1,2], B F Felemban[1] , A Alharthi[1], S Almalki[1], E Fathallah [3,4] , A A Elsherbiny[2] and H Eleashy[5]

[1]Department of Mechanical Engineering, College of Engineering, Taif University, Taif 21974
[2]Production and Mechanical Design Department, Faculty of Engineering, Mansoura University, Mansoura 35516, Egypt
[3]Civil Engineering Department, M.T.C. Kobry Elkobba - Cairo, Egypt
[4]Ships and Submarines Engineering Department, Military Technical College, Cairo, Egypt.
[5]Mechanical Engineering Department, Faculty of Engineering & Technology, Future University in Egypt, Cairo, Egypt

E-mail: saidhabib2000@hotmail.com

Abstract. The connecting rod is an important component of the engine. It conveys the kinetic energy from the piston to the crankshaft. All cars and aircraft engines contain at least one connecting rod, which differs from one motor to another in terms of length, size and shape. Hence, it is subjected to massive alternating load. This research aims to improve the connecting rod design by reducing its mass without sacrificing durability and safety especially for aircraft applications. Therefore, a static stress analysis is carried out on forged steel connecting rod using ANSYS APDL. Geometric modelling of the connecting rod was created using ANSYS APDL. Additionally, von-Mises stress and strain, principal stresses and strains, shear stress and the deflation results of the connecting rod are investigated. The results showed a great opportunity for mass weight reduction. Thus, a dimensional structural mass optimization was performed. The optimization results were promising, which reduced the mass by 55.13% (in the tensile case) and 56.7% (in the compression case) from the initial design. Therefore, the efficiency of aircraft engine can be maximized.

1. Introduction:

One of the most critical parts of the internal combustion engines is the connecting rod which connects the piston to the crankshaft. In general, connecting rods are made of steel for vehicles and aircraft engines. But, it can be made from different materials such as Titanium for high-performance engines, or Aluminum (for the ability to absorb high impact and lightness at the expense of durability) or Cast iron for applications such as motor scooters. The connecting rod is under reciprocating load and due to this is under an incredible tensile and compression stress at every rotation. One of the most common engine failure cases is the connecting rod failure, which can result from a physical defect in the rod, lubrication, or bolt defects. Often these failures happen at competitive automobile events. But, not on production cars during normal daily driving, which rarely occurs, due to the greater safety factor in parts production, and quality control is often more systematic [1, 2]. The demand for robust and alternative materials has grown in the industry fields. A technique of hybridization involves a combination of two or more reinforcements to obtain better mechanical properties, such as strength, stiffness, higher strength to weight ratio, etc. And by combining two or more low-cost materials with different properties, the hybrid materials are formed. These advanced materials are used for high-strength; light-weight applications in automobiles, aerospace, etc. several techniques are used to create hybrid metal matrix composites such as stir cum squeeze, casting process, and stir casting process [3].

In the early years, connecting rod optimization has started. Consumers are looking for more robust and safer products at a reasonable price. However, the industry is looking for less time and cost production. The best values for these variables that achieve all these constraints can be determined by the optimization process, making it essential and primarily in the automotive industry. The car performance is affected by the design and weight of the connecting rod. Thus, it also affects car manufacture credibility. By considering the weight reduction structural factors during optimization, the component can be lighter and maintain higher strength, which will create striking success in the automotive and manufacturing industry. The benefits of connecting rod optimization go back to the consumers themselves. Among the key goals are to boost the engine's efficiency and enhance the product that guarantees human protection.[4]. The connecting rod can bear both static and dynamic loads. The compression and tensile stresses on the connecting rod are generated respectively by the pressures exerted by the combustion gases and the components of the inertial movement [5, 6]. In case of faulty connection or fatigue, connecting rods fail. Also, connecting rods may fail due to failure of loading, irregular adjustments of screws [7]. Connecting rod must resist the applied tensile stresses. consequently, some design techniques, material selection, and fatigue tests have been presented [8].

Failure of connecting rod is attributed to the availability of strength that is required to withstand the applied stresses. But by extending the life cycle by increasing the strength we can overcome it. Sathish et al.[1], performed static stress analysis based on the finite element method to AA2014, AA6061 and AA7075 aluminum alloy materials using ANSYS, and found that the AA2014 is the less weight and better stiffness which has the minimum values of equivalent stress, equivalent elastic strain, and the total deformation. Gopinath et al. [4], performed static analysis based on finite element analysis to forged steel, aluminum and titanium connecting rod. Further, a weight reduction by topology optimization technique on forged steel connecting rod is carried out. Rezvani et al. [9], studied the catastrophic joint deformation failure of the 645E3B diesel engine connecting rod. The findings confirm that the failure causes are assumed to be the hydro-lock condition due to the splash of water within the ignition chamber and the higher-pressure proportion. Abad et al. [10], performed dynamic load analysis as well as optimization of connecting rod. Lee et al. [11], investigated the buckling sensitivity by reducing the connecting rod weight. And found that in buckling, the stress sensitivity is more than or equal to fatigue and yield stress. Kreculj et al. [12], analyzed the impact load effect on the structure of aircraft. The accumulated impact damage and the impact damage effect are discussed. Additionally, Ranjan Pani et al. [13], performed a theoretical and a numerical buckling failure analysis and material selection for the 645E3b engine connecting rod. The theoretical part is taken to calculate the buckling load and stress using the merchant-Rankine approach and the slider-crank mechanism approach. The numerical analysis is done by ANSYS to validate the results. And conclude that, a proper buckling safety factor should be taken to avoid the buckling failure. The Al-2024-T6 is not ideal for heavy-duty diesel engines due to the lower buckling strength compared to 42CrMo4. Furthermore, Sharma et al. [14], carried out analysis and modeling of carbon steel and aluminum boron carbide connecting rod and found that the nearest working factory of safety to the theoretical factory of safety is the aluminum boron carbide connecting rod which has 48.55% more stiffness and 10.35% less stress. Pathade et al. [15], performed a finite element analysis (FEA) on the connecting rod using both ANSYS and pro-wild fire software and found that the small end stresses are greater than in the bigger end. In addition, concluded that the chance of the connecting rod failure may be at the fillet section of both ends. Bansal et al. [16], carried out a dynamic and a static FEA on aluminum alloy connecting rod. The static load analysis preformed for stress analysis, optimization and to determine the connecting rod von-Mises stresses. Ahmed et al. [17], carried out FEA on a connecting rod with three aluminum alloys materials (AA2014, AA7075, and AA6061) and carbon fiber. Bin et al. [18], performed FEA on a connecting rod to investigate the stress distribution and fatigue life cycle. Gautam et al. [19], carried out a static stress analysis based on FEA on SS304 connecting rod used in Cummins NTA885BC engine. Also, He et al. [20], carried out failure analysis of a diesel engine connecting rod. The reason for the connecting rod's failure was the high-stress concentration/high-stress level and lower yield strength. Londhe et al.[21], performed FEA and an experimental study of the connecting rod and found that both the experimental and the simulation results of the fatigue and static strain matched, thereby validating the FEA. Moreover, Rabb [22], studied the fatigue failure of the connecting rod. Similarly, Rakic et al. [23], predicted the failure of a connecting rod based on the FEA, which showed the concentration of maximum stress applied at position of original fracture. Witek et al. [24], conducted stress analysis on connecting rod using ANSYS. They observed that maximum principal stress can be found at zone near the bolt hole where the crack originated and it exceeded the fatigue limit of 42CrMo4 steel. Seralathan et al.[25], performed static stress analysis based on the FEA to different types of materials using ANSYS finite element code and found that, the A356-5%SiC-10% Flyash stir cum squeeze casting material has the minimum values of equivalent stress, equivalent elastic strain, and total deformation. A lot of research deals with weight loss [26, 27].

In this paper, the structural design optimization to reduce the weight of forged steel connecting rod in aircraft engines using a finite element method is performed. The connecting rod model is created using ANSYS APDL. The von-Mises stress, strain, shear stress and the deflation results of the connecting rod are investigated.

2. Finite element modeling and optimization

The FEA is widely used for solving different problems of engineering and predicting the behavior of structural elements as in [28-33]. FEA is the most significant applied technique for analyze engineering structures according to specific design considerations. It dives the real object into a large number small units called "elements" for dynamic and static analysis of simple to complex models in the presence of varied design constraints. Further checks could be done to improve a design for optimum performance and life about design failure [34]. The components of the connecting rod are illustrated in ***Figure 1***. Geometry and dimensions of the connecting rod are shown in ***Figure 2***. The model was crated and mapped in ANSYS software package by using ANSYS Parametric Design Language (APDL). The accuracy of the results is controlled by the element type and meshing of the model, which is responsible for dividing the model into a number of small elements. The smaller the elements size the more accurate the results. In the present paper, the model is meshed using Plane183 element as shown in ***Figure 3***. The total number of elements and nodes are (1157) and (3949), respectively. The mechanical properties for the Forged steel are as listed in **Table *1***.

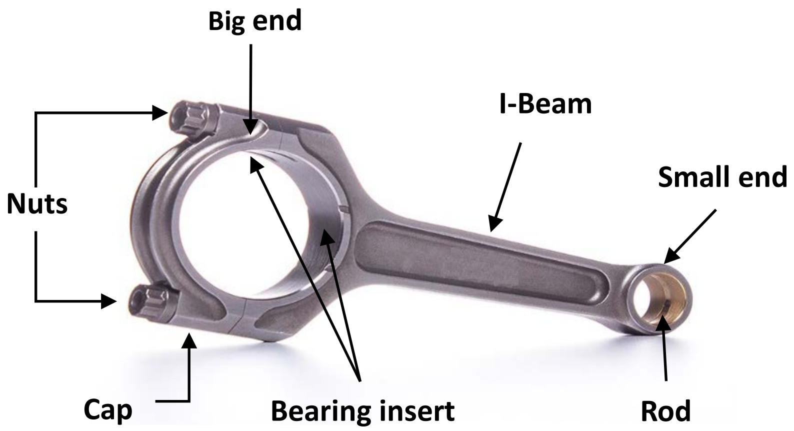

Figure 1: Connecting rod components.

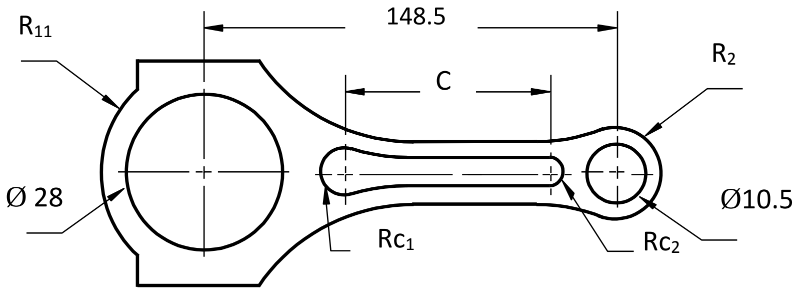

Figure 2: Connecting rod geometry and dimension (all dimensions are in mm).

Table 1: Mechanical properties of Forged Steel.

Young's Modulus, E	200GPa
Poisson's ratio, υ	0.3
Density, ρ	7850 Kg/m^3
Shear Modulus, G	78 GPa
Tensile Strength, σ_U	892.63 MPa
Yield Strength, σ_y	648.06 MPa

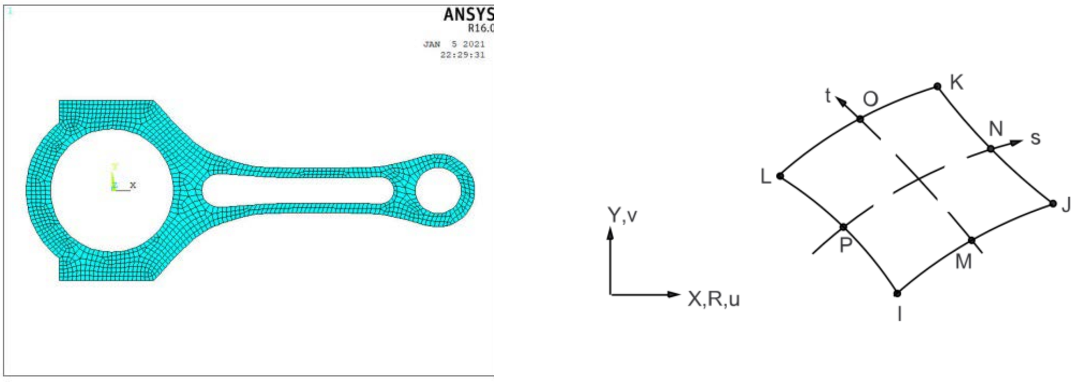

(a) (b)

Figure 3: Meshing and element type (a) Connecting rod mesh and (b) the geometry of plane183 element.

2.1 Boundary condition

The connecting rod is subject to two types of loads, the first being in compression and the other being in tension. In the tension case, the load is applied on the right half of small end at 120 degrees and the big end is fully fixed as shown in ***Figure 4*** (a). In the compression case: the load is applied on the left half of the small end at 120 degrees and the big end is fully fixed as shown in ***Figure 4*** (b). The chosen pressure value is 24.2 MPa [35].

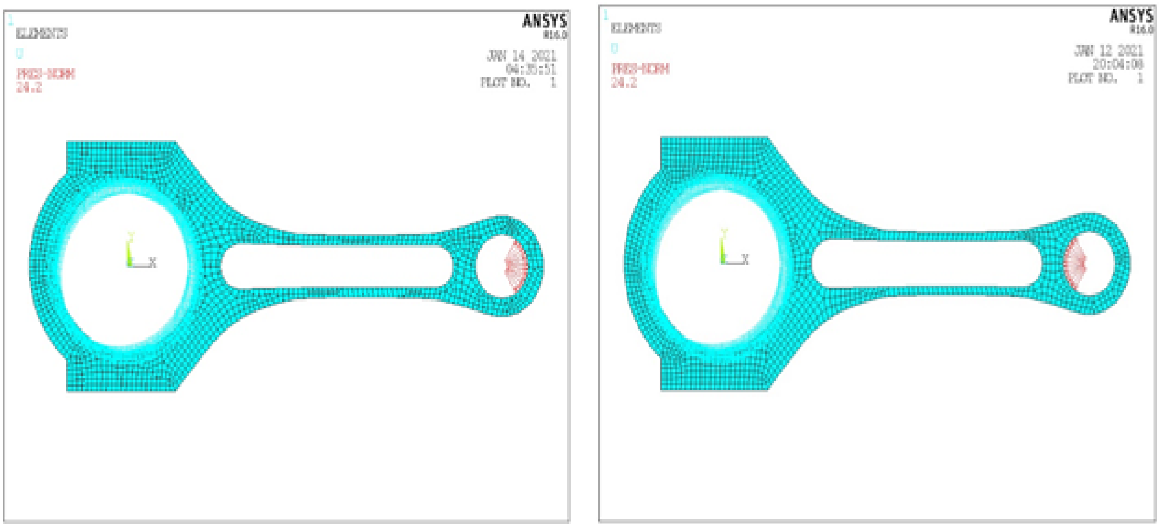

(a) (b)

Figure 4: Boundary condition of connecting rod (a) for tension (b) for compression.

2.2 Optimization statement

Design Optimization is a crucial mathematical method used in engineering and many other fields. Generally, it is a process of finding the optimal value of one or many design parameter that meets the system requirement and achieve the best performance [36]. Hence, the design optimization of the connecting rod is to minimize the mass of the connecting rod while bearing the compressive and the tension load acting on it [4]. The design optimization flow chart is shown in ***Figure 5***.

2.3 Objective function

The objective function f(x) is the parameter that desired to be minimized or maximized. In this paper the objective function is to minimize the connecting rod mass:

$$f(x) = minimaze\ the\ connecting\ rod\ mass(Kg)$$

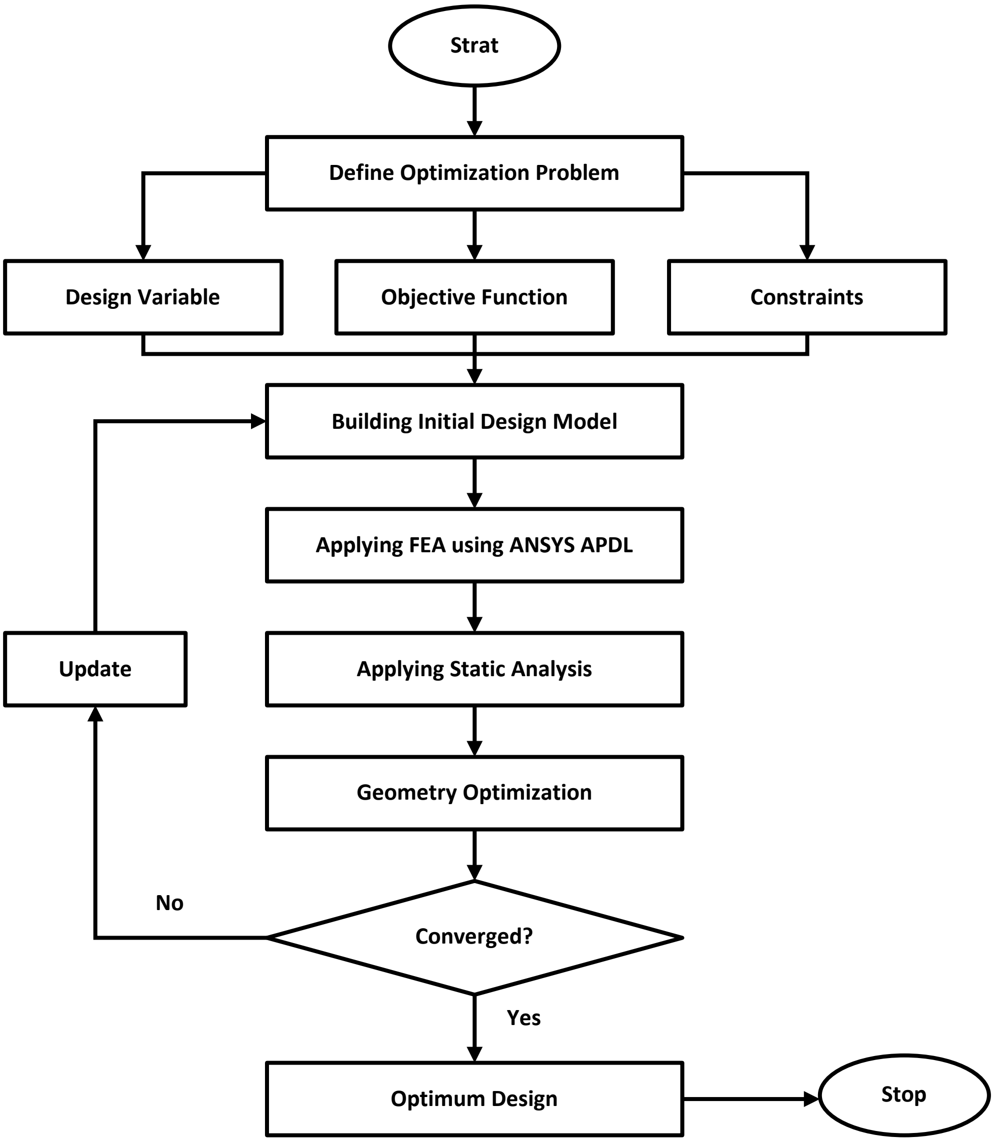

Figure 5: *Design optimization flow Chart*

2.4 Design constraints:

Design constraints are the range that parameters cannot go over or below it to avoid failure and meet the requirements. In this paper, constraints are characterized into two types: material and side constraints.

Material constraints:

To avoid connecting rod failure the following constraints must be satisfied:

1- The deflection $(\boldsymbol{\delta})$ of the connecting rod must not exceed the allowable deflection $(\boldsymbol{\delta_a})$ Mathematically:

$$\delta < \delta_a$$

2- The von-Mises stress $(\boldsymbol{\sigma})$ must not exceed the allowable stress $(\boldsymbol{\sigma_a})$ Mathematically:

$$\sigma < \sigma_a$$

Side constraints:
Side constraints are identified as the range limits of the dimensions parameter as listed in the Table 2.

Table 2: Side Constraints

	Lower limit	**Upper limit**
Outer big end (R_1)	${R_1}^L$	${R_1}^U$
Outer small end (R_2)	${R_2}^L$	${R_2}^U$
Big circle (Rc_1)	${Rc_1}^L$	${Rc_1}^U$
Small circle (Rc_2)	${Rc_2}^L$	${Rc_2}^U$
Center distant between big and small circle (C)	C^L	C^U
Connecting rod thickness (t)	t^L	t^U

3. Results and discussion

Based on Finite element analysis (FEA) and ANSYS Parametric Design Language (APDL), dimensional structural mass optimization is performed on forged steel connecting rod for aircraft engines under 24.2 MPa tension and compressive pressure.

3.1 Real model results

Numerical static stress analysis of forged steel connecting rod under 24.2 MPa tensile and compression pressure is obtained for a real model. Additionally, von-Mises stress, shear stress, total deformation, von-Mises strain and principal stresses and strains of the connecting rod are obtained in both tension and compression cases as shown in ***Figure 6*** and ***Figure 7***, respectively.

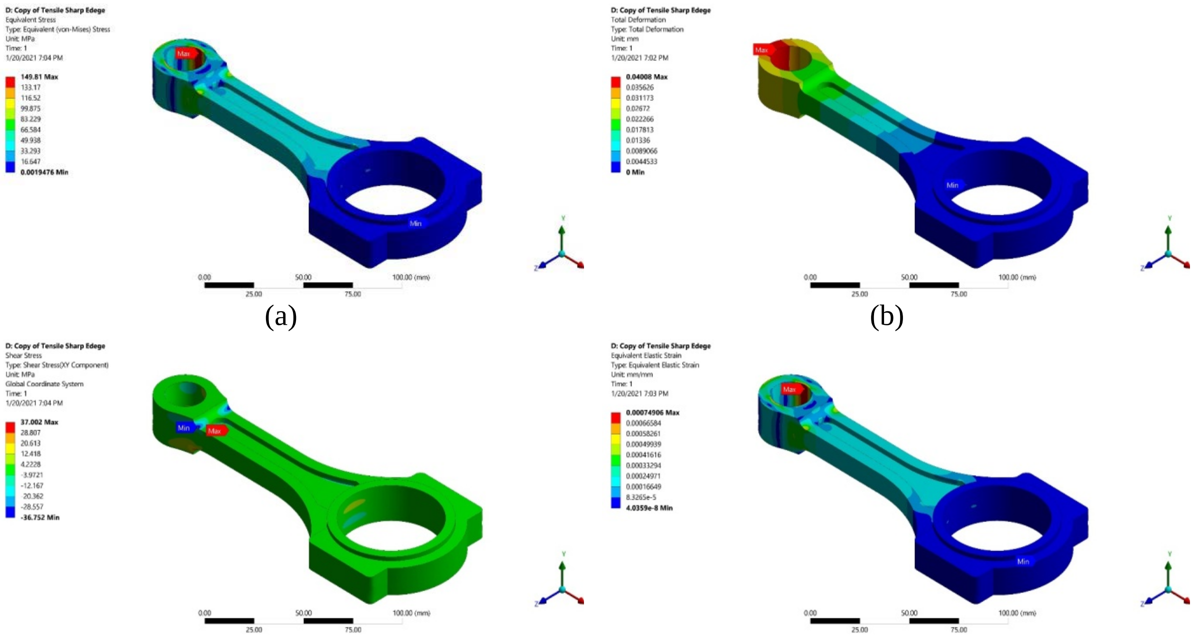

(a) (b)

(c) (d)

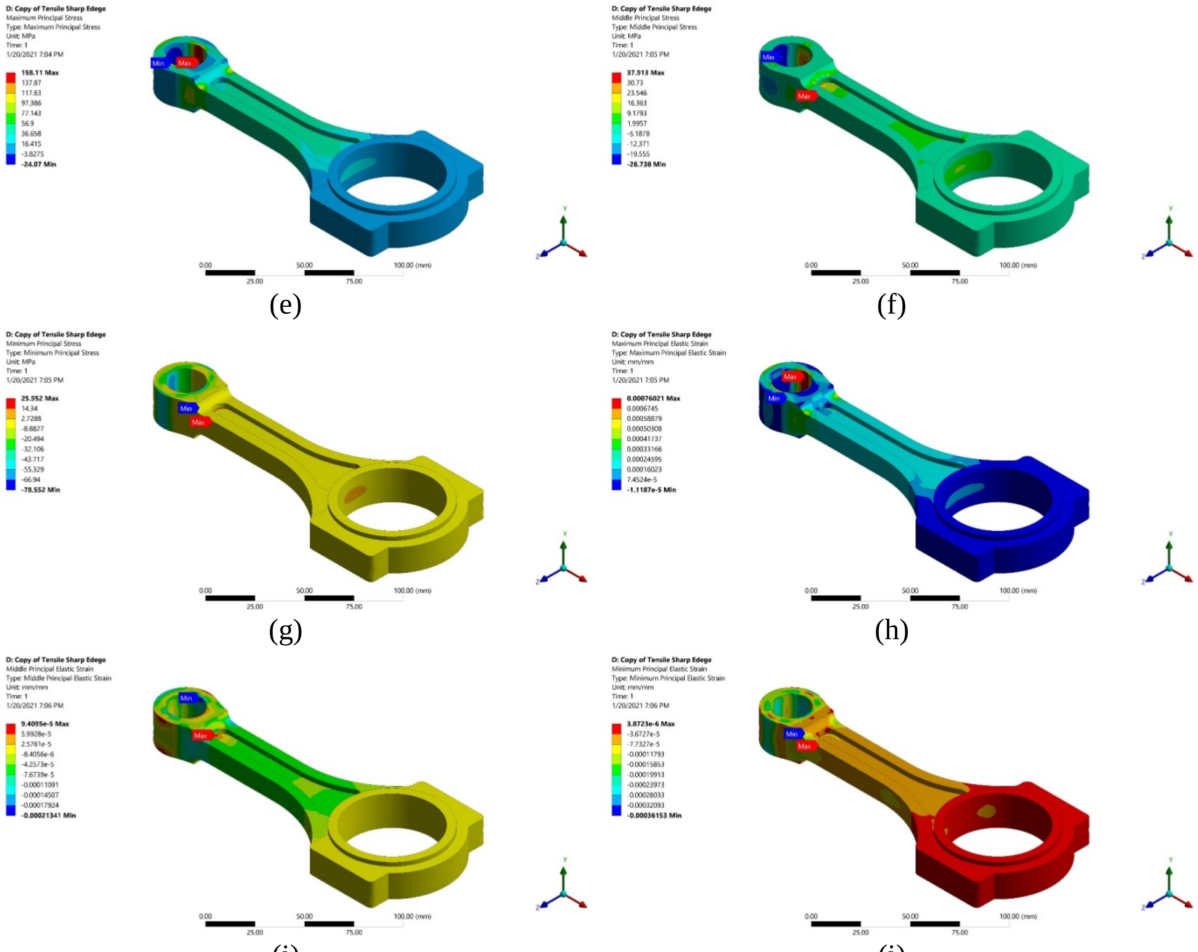

(e) (f)

(g) (h)

(i) (j)

Figure 6: Connecting rod tensile case results of (a) von-Mises stress, (b) Total deformation (c) Shear stress, (d) von-Mises strain, (e) 1st Principal stress (f) 2nd Principal stress (g) 3rd Principal stress and (h-j) 1st, 2nd and 3rd Principal strain.

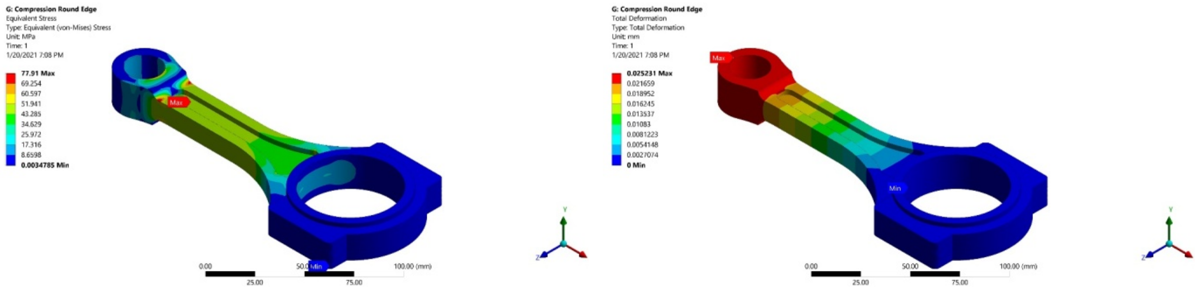

(a) (b)

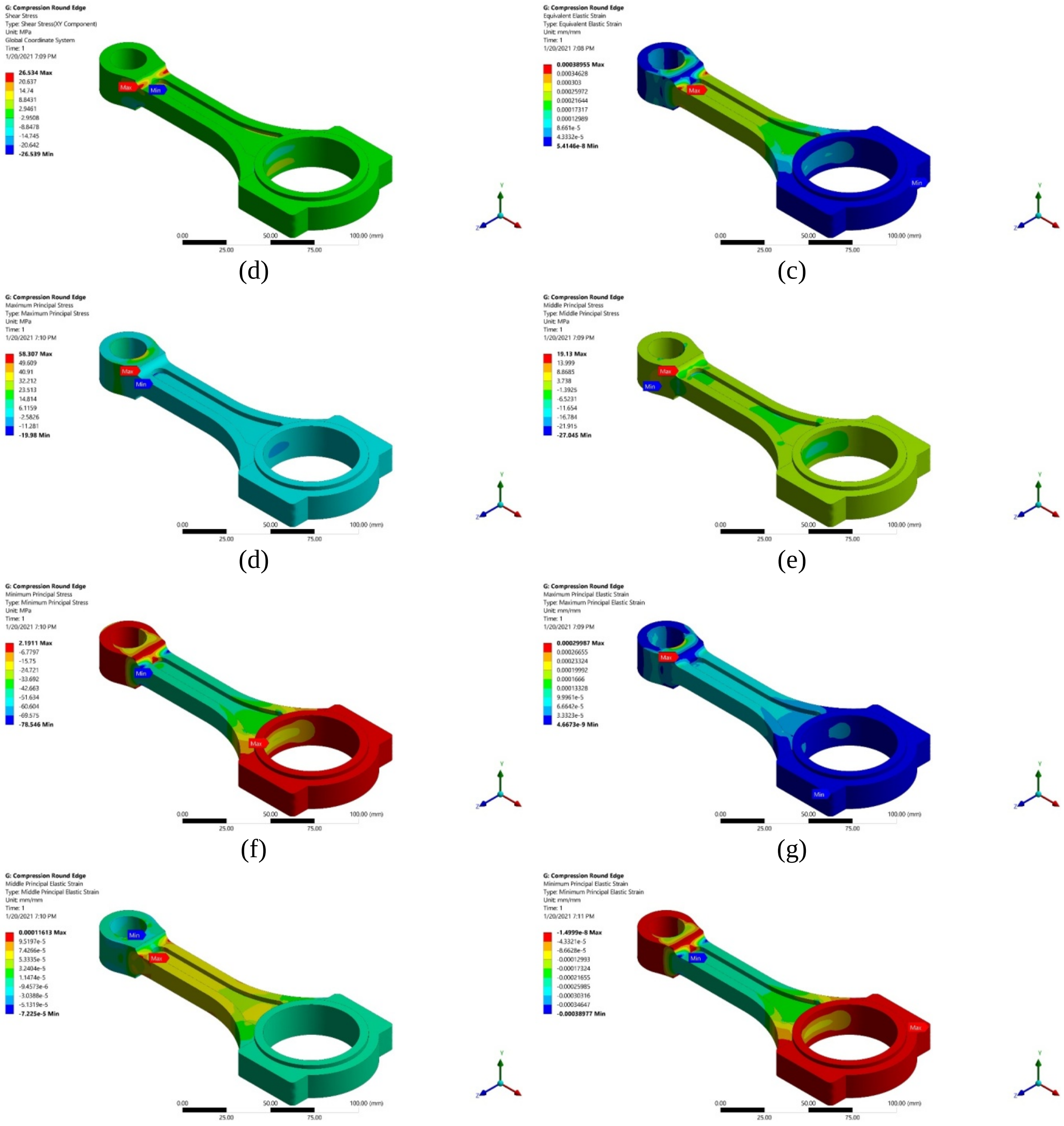

(d) (c)

(d) (e)

(f) (g)

(h) (i)

Figure 7: Connecting rod compression case results of (a) von-Mises stress, (b) Total deformation, (c) Shear stress, (d) von-Mises strain, (e) 1st Principal stress (f) 2nd Principal stress (g) 3rd Principal stress and (h-j) 1st, 2nd and 3rd Principal strain.

3.2 Optimized model results

The aim of the optimization is to reduce the connecting rod mass while meeting all the material and the side constraints. Numerical static stress analysis of forged steel connecting rod under 24.2 MPa tensile and compresion pressure is performed for the proposed optimized model. Also, von-Mises stress, shear stress, total deformation, von-Mises strain and prrincple stresses and strains of the connecting rod are obtained for the proposed optimized model in both tension and compression cases as demonstrated in ***Figure 8*** and ***Figure 9*** repectively. Detailed numerical results for real and optimized model can be summarized in ***Table 3***

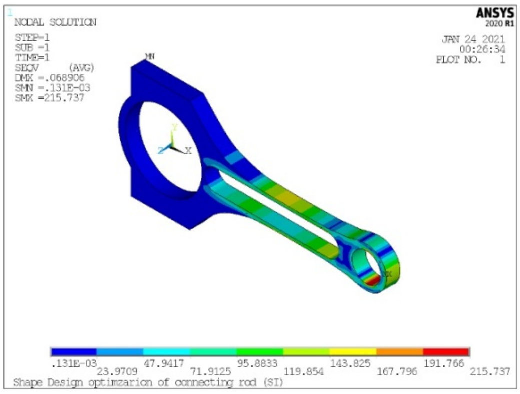
NODAL SOLUTION
STEP=1
SUB =1
TIME=1
SEQV (AVG)
DMX =.068906
SMN =.131E-03
SMX =215.737
ANSYS
2020 R1
JAN 24 2021
00:26:34
PLOT NO. 1
MN
MX
Y
Z
X
.131E-03
23.9709
47.9417
71.9125
95.8833
119.854
143.825
167.796
191.766
215.737
Shape Design optimzarion of connecting rod (SI)

(a)

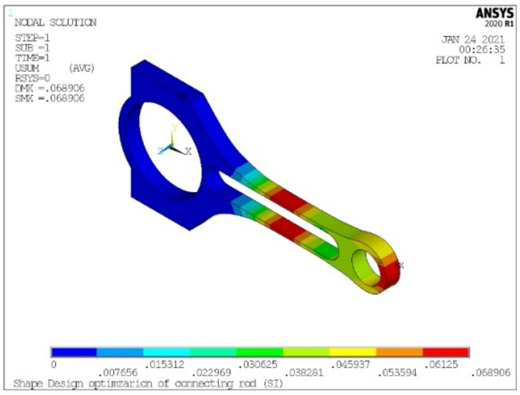
NODAL SOLUTION
STEP=1
SUB =1
TIME=1
USUM (AVG)
RSYS=0
DMX =.068906
SMX =.068906
ANSYS
2020 R1
JAN 24 2021
00:26:35
PLOT NO. 1
MN
MX
Y
Z
X
0
.007656
.015312
.022969
.030625
.038281
.045937
.053594
.06125
.068906
Shape Design optimzarion of connecting rod (SI)

(b)

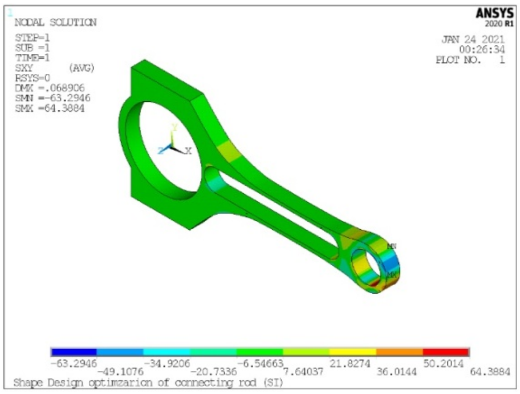
NODAL SOLUTION
STEP=1
SUB =1
TIME=1
SXY (AVG)
RSYS=0
DMX =.068906
SMN =-63.2946
SMX =64.3884
ANSYS
2020 R1
JAN 24 2021
00:26:34
PLOT NO. 1
MN
MX
Y
Z
X
-63.2946
-49.1076
-34.9206
-20.7336
-6.54663
7.64037
21.8274
36.0144
50.2014
64.3884
Shape Design optimzarion of connecting rod (SI)

(d)

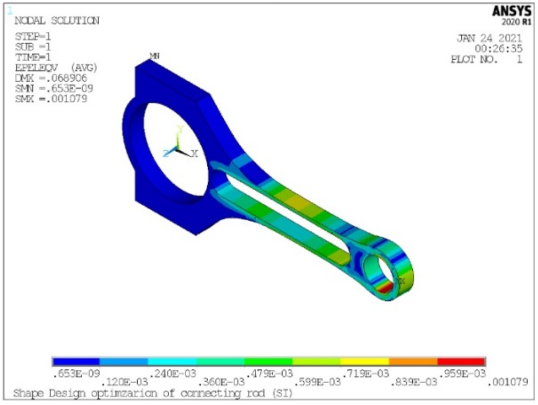
NODAL SOLUTION
STEP=1
SUB =1
TIME=1
EPELEQV (AVG)
DMX =.068906
SMN =.653E-09
SMX =.001079
ANSYS
2020 R1
JAN 24 2021
00:26:35
PLOT NO. 1
MN
MX
Y
Z
X
.653E-09
.120E-03
.240E-03
.360E-03
.479E-03
.599E-03
.719E-03
.839E-03
.959E-03
.001079
Shape Design optimzarion of connecting rod (SI)

(c)

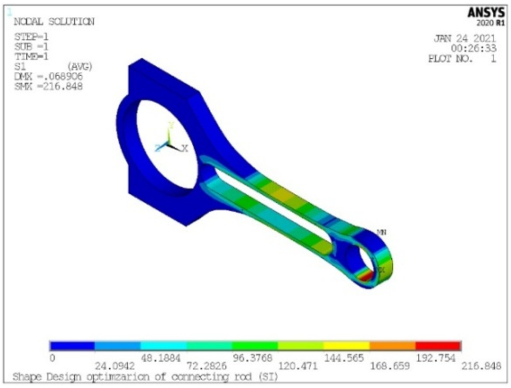
NODAL SOLUTION
STEP=1
SUB =1
TIME=1
S1 (AVG)
DMX =.068906
SMX =216.848
ANSYS
2020 R1
JAN 24 2021
00:26:33
PLOT NO. 1
MN
MX
Y
Z
X
0
24.0942
48.1884
72.2826
96.3768
120.471
144.565
168.659
192.754
216.848
Shape Design optimzarion of connecting rod (SI)

(d)

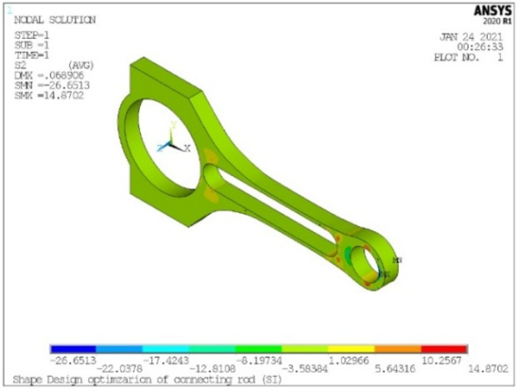
NODAL SOLUTION
STEP=1
SUB =1
TIME=1
S2 (AVG)
DMX =.068906
SMN =-26.6513
SMX =14.8702
ANSYS
2020 R1
JAN 24 2021
00:26:33
PLOT NO. 1
MN
MX
Y
Z
X
-26.6513
-22.0378
-17.4243
-12.8108
-8.19734
-3.58384
1.02966
5.64316
10.2567
14.8702
Shape Design optimzarion of connecting rod (SI)

(e)

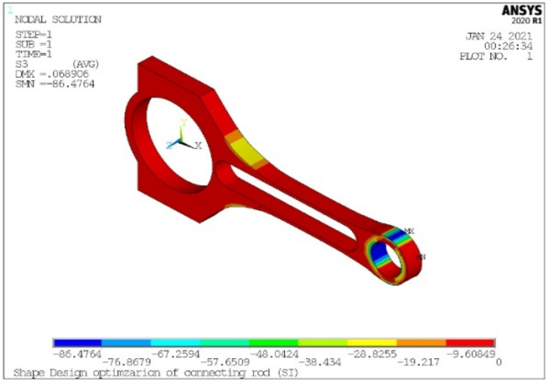
NODAL SOLUTION
STEP=1
SUB =1
TIME=1
S3 (AVG)
DMX =.068906
SMN =-86.4764
ANSYS
2020 R1
JAN 24 2021
00:26:34
PLOT NO. 1
MX
MN
Y
Z
X
-86.4764
-76.8679
-67.2594
-57.6509
-48.0424
-38.434
-28.8255
-19.217
-9.60849
0
Shape Design optimzarion of connecting rod (SI)

(f)

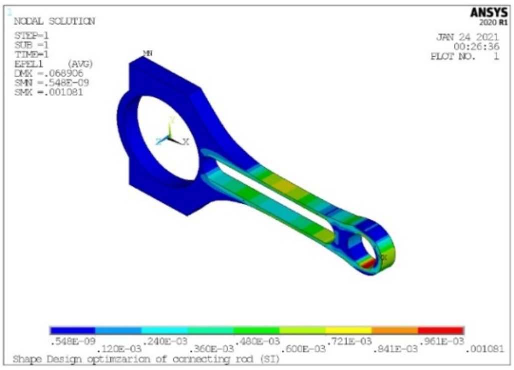
NODAL SOLUTION
STEP=1
SUB =1
TIME=1
EPEL1 (AVG)
DMX =.068906
SMN =.548E-09
SMX =.001081
ANSYS
2020 R1
JAN 24 2021
00:26:36
PLOT NO. 1
MN
MX
Y
Z
X
.548E-09
.120E-03
.240E-03
.360E-03
.480E-03
.600E-03
.721E-03
.841E-03
.961E-03
.001081
Shape Design optimzarion of connecting rod (SI)

(g)

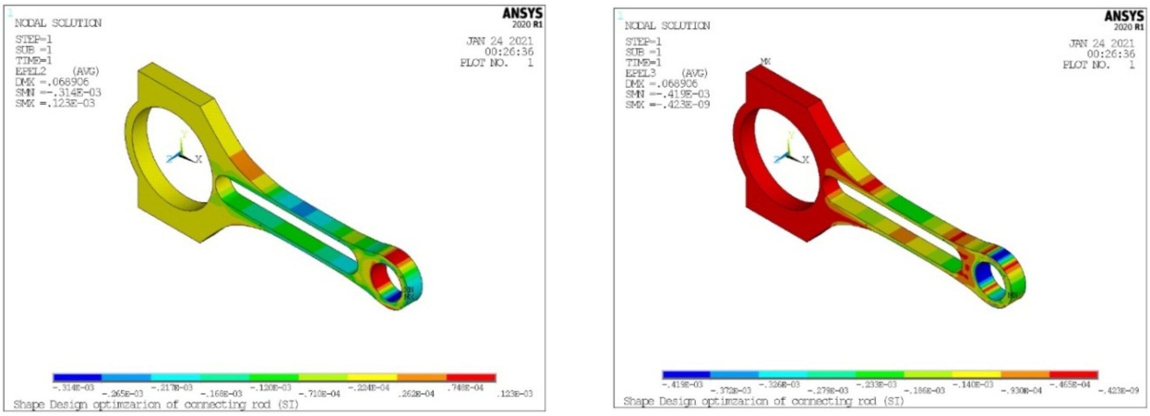

(h) (i)

Figure 8: Connecting rod optimized (tensile case) results of (a) von-Mises stress, (b) Total deformation, (c) Shear stress, (d) von-Mises strain, (e) 1st Principal stress (f) 2nd Principal stress (g) 3rd Principal stress and (h-j) 1st, 2nd and 3rd Principal strain.

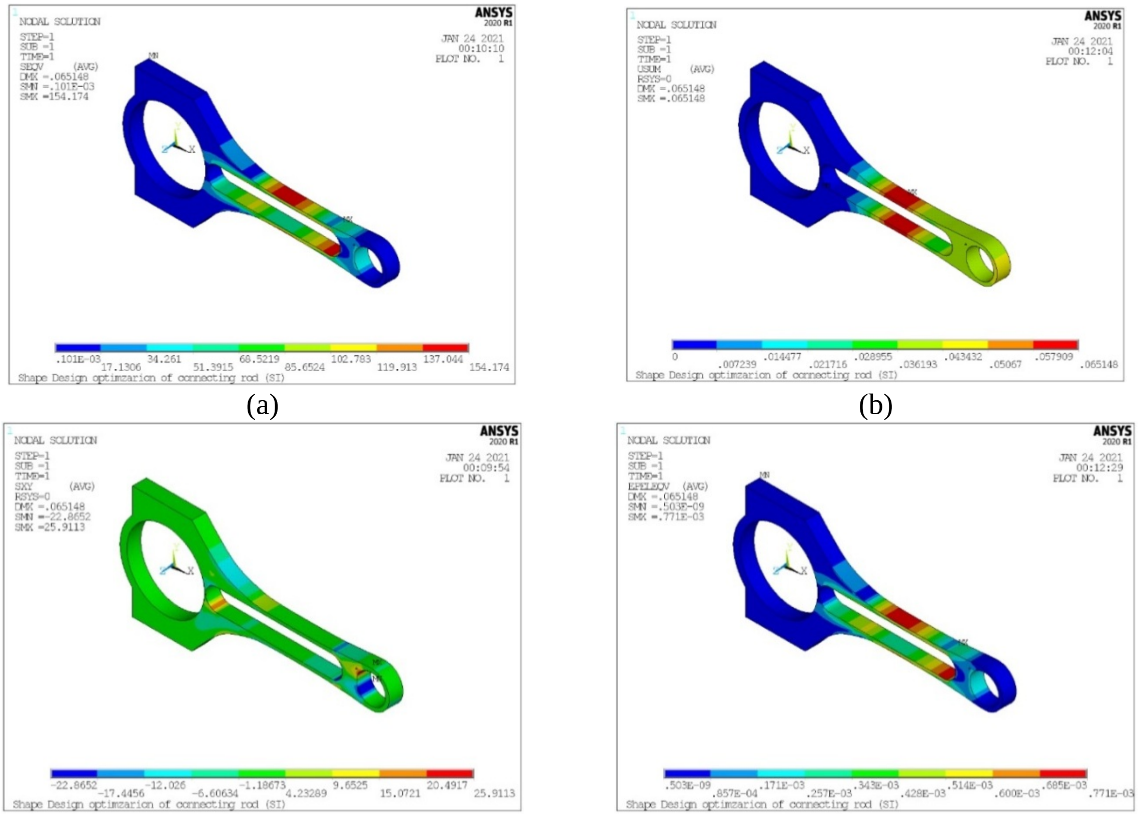

(a) (b)

(d) (c)

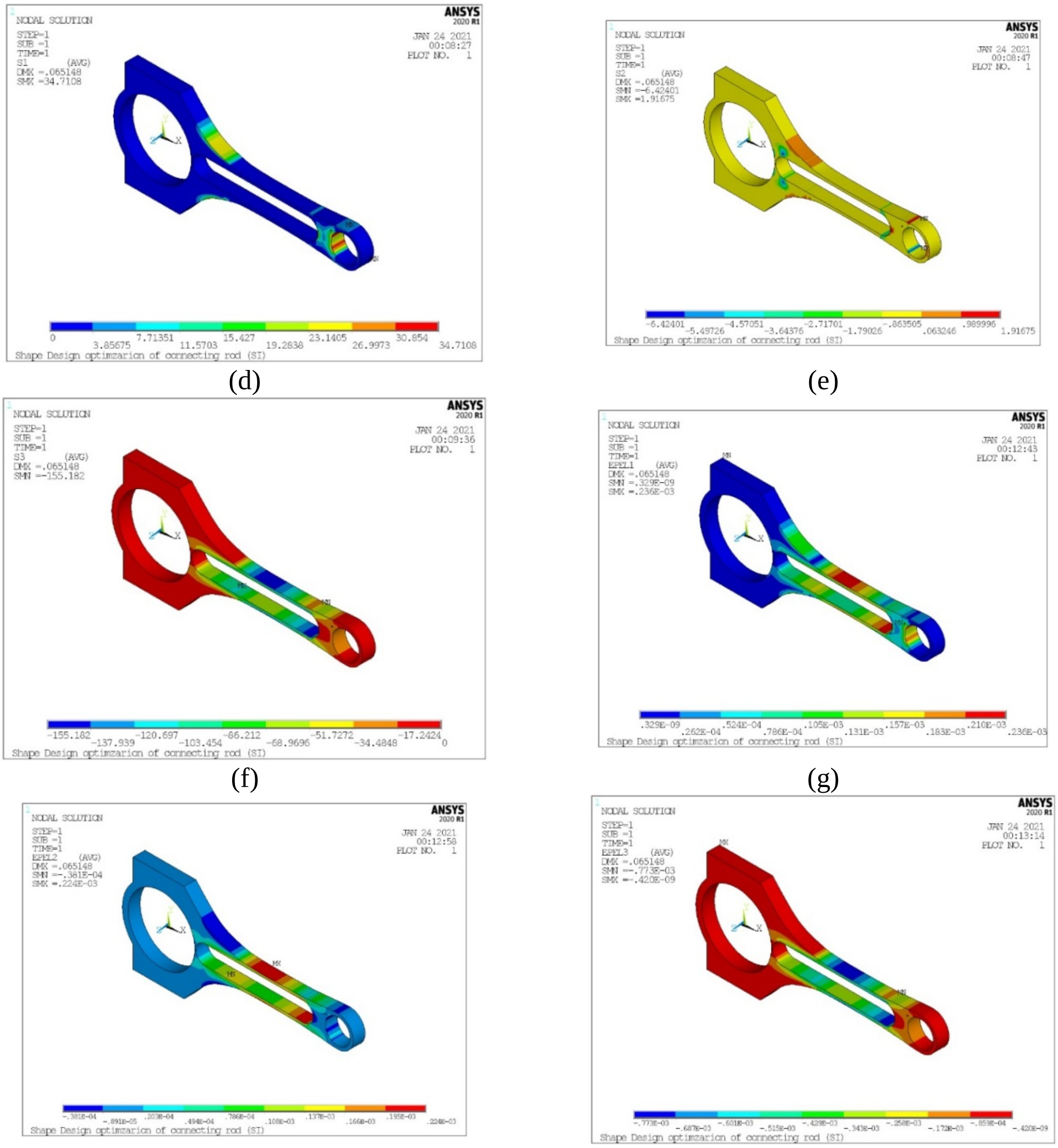

(d) (e)

(f) (g)

(h) (i)

Figure 9: Connecting rod optimized (Compression case) results of (a) von-Mises stress, (b) Total deformation, (c) Shear stress, (d) von-Mises strain, (e) 1st Principal stress (f) 2nd Principal stress (g) 3rd Principal stress and (h-j) 1st, 2nd and 3rd Principal strain.

Table 3.Detailed numerical results for real and optimized model

			von-Mises stress (MPa)	Deflation (mm)	Shear stress (MPa)	von-Mises elastic strain	Principals stresses (MPa)	Principals strains
Real model	Tension case	*Max. Value*	148.81	0.04	37	7.5e-4	--	--
		Position	small end	small end	I-beam	small end	--	--
		Min. Value	2×10^{-3}	0	-36.75	4.04×10^{-8}	--	--

		Values	--	--	--	--	158.1, 37.91 and -78.55	7.6×10^{-4}, -2.13×10^{-4} and -3.6×10^{-4}
		Figure	6 (a)	6 (b)	6 (c)	6 (d)	6 (e-g)	6 (h-j)
	Compression case	*Max. Value*	77.91	0.03	26.53	3.9×10^{-4}	--	--
		Position	I-beam	small end	I-beam	I-beam	--	--
		Min. Value	3.5×10^{-3}	0	-26.53	5.4×10^{-8}	--	--
		Values	--	--			58.3, -27and -78.55	3×10^{-4}, 1.2×10^{-4} and -4×10^{-4}
		Figure	7 (a)	7 (b)	7 (c)	7 (d)	7 (e-g)	7 (h-j)
Optimized model	Tension case	*Max. Value*	215.74	0.07	64.4	1.1e-3	--	--
		Position	small end	small end	small end	small end	--	--
		Min. Value	1.3×10^{-4}	0	-63.3	6.53×10^{-10}	--	--
		Values	--	--	--	--	216.8 , -26.7 and -86.5	1.1×10^{-3}, 3.14×10^{-4} and -4.2×10^{-4}
		Figure	8 (a)	8 (b)	8 (c)	8 (d)	8 (e-g)	8 (h-j)
	Compression case	*Max. Value*	154.2	0.065	26	7.7e-4	--	--
		Position	I-beam	middle of connecting rod	small end	I-beam	--	--
		Min. Value	4	0	-23	5×10^{-10}	--	--
		Values	--	--	--	--	34.71, -6.42 and -155.2	2.4×10^{-4}, 2.24×10^{-4} and -7.73×10^{-4}
		Figure	9 (a)	9 (b)	9 (c)	9 (d)	9 (e-g)	9 (h-j)

4. Comparison between real and optimized model

From the previous results, structural optimization significantly minimizes the mass of the connecting rod by 55.13 % in the tensile case and 56.7 % in the compression case, which in turn reduces the production time and cost. Table 4 clarifies a comparison between the real and the optimized results of the connecting rod.

Table 4: Comparison between the real and optimized results.

Parameter	Real Model	Optimum Model

		Tensile	Compression	Tensile	Compression
1	von-Mises Stress (MPa)	148.81	77.91	215.7	154.2
2	Total Deformation (mm)	0.04	0.03	0.069	0.065
3	Factor of Safety (F.S)	4.35	8.32	3	4.2
3	Mass (Kg)	0.64		0.29	0.28
4	Volume (mm^3)	81112		36391	35233
5	Weight reduction (%)	-		55.13	56.7

5. Conclusion

In this paper, a static stress analysis was performed on forged steel connecting rod in aircraft engines under 24.2 MPa tensile and compression pressure using ANSYS APDL. The maximum and the minimum of von-Mises stress and strain, the principal stresses and strains, shear stress, and the deflection were investigated. The results show a significant opportunity for weight reduction optimization. Thus, a dimensional structural mass optimization was carried out to minimize the connecting rod's mass after performing static stress analysis. That, in turn, will enhance the performance of aircraft engines. The optimization results show notable weight reduction of the connecting rod by 55.13 % (in the tensile case) and 56.7 % (in the compression case) from the initial design. However, fatigue analysis for a connecting rod will be considered in further work.

Funding: This research received no external funding.
Acknowledgments: The authors are grateful to Taif University (Taif, KSA), Mansoura University (Mansoura, Egypt), Military Technical College (Cairo, Egypt) and Future University in Egypt (Cairo, Egypt) for providing all the required facilities to carry out the present research.
Conflicts of Interest: The authors declared no conflicts of interest.

Biography

Associate Professor Mahmoud M. K. Helal, received his B.Sc. and MSc. degrees from Production and Mechanical Design Department, faculty of Engineering, Mansoura University in 2000 and 2005, respectively. In 2011 he received his Ph.D. degree from Harbin Institute of Technology (HIT). He works as an assistant professor in the Production and Mechanical Design Department at Mansoura University. Dr. Helal's research interests lie in the structural optimization, the strength of the materials; MEMS design assembly, micromanipulation robot and solid mechanics.

Assistant Professor Bassem F. Felemban, revived his B.Sc. Degree from Production and Mechanical Design Department, King Abdelaziz University in 2009. Then he received the MSc. and Ph.D. degrees from Mechanical Engineering, University of Central Florida (UCF). He is working as an assistant professor in the Production and Mechanical Design Department at Taif University. Dr. Bassem F. Felemban works as a member of Mechanical of Materials Research Group at UCF.

Abdullah Alharthi, studied Mechanical Engineering at department of Mechanical Engineering, Faculty of Engineering, Taif University. Email: eng.abdullah.harthi@gmail.com.

Sari Almalki, is studied Mechanical Engineering at department of Mechanical Engineering, Faculty of Engineering, Taif University. Email: sariayed.3@gmail.com

Assistant Professor Elsayed Fathallah, received his bachelor and master degrees in Civil Engineering from Civil Engineering Department from Military Technical College in 1999 and 2007, respectively. In 2015 he received his Ph.D. degree from Harbin Engineering University, College of Aerospace and Civil Engineering. He works as an assistant professor at both Civil Engineering and Ships and Submarines

Engineering Department, Military Technical College. His research focuses on strength of the material and structural optimization.

Abdallah A. Elsherbiny, received his B.Sc., MSc. degrees from Production and Mechanical Design Department, faculty of Engineering, Mansoura University**.** He works as an assistant lecture in the same department.

Assistant Professor, Hassan M. S. Eleashy, received his B.Sc., MSc. and Ph.D degrees from Production and Mechanical Design Department, faculty of Engineering, Mansoura University in 2000, 2006, and 2014 respectively. He works as an assistant professor in the Mechanical Engineering Department at Future University in Egypt. Dr. Eleashy research interests lie in the mechanism design, structural synthesis of robots, planetary gear trains and stress analysis.

References

[1] Sathish, T., Kumar, S.D. and Karthick, S., 2020. Modelling and analysis of different connecting rod material through finite element route. *Materials Today: Proceedings*, ***21*,** pp.971-975.

[2] Dinesh Kumar, S. and Purushothaman, K., 2019. Enhancement of thermal conductivity in a plate heat exchanger by using nanoparticles CNT, Al2O3, surfactant with de-ionised water as a coolant. *International Journal of Ambient Energy*, pp.1-4.

[3] Ranganathan, S., Kuppuraj, S., Soundarrajan, K. and Perumal, A., 2019. *Design and Analysis of Hybrid Metal Matrix Composite Connecting Rod via Stir/Squeeze Casting Route* (No. 2019-28-0113). SAE Technical Paper.

[4] Gopinath, D. and Sushma, C.V., 2015. Design and optimization of four wheeler connecting rod using finite element analysis. *Materials Today: Proceedings*, ***2*****(4-5)**, pp.2291-2299.

[5] Heywood, J.B., 2018. Internal Combustion Engine Fundamentals (2nd edit). *McGrow-Hill Education*.

[6] Shenoy, P.S., 2004. *Dynamic load analysis and optimization of connecting rod* (Doctoral dissertation, University of Toledo).

[7] Ilman, M.N. and Barizy, R.A., 2015. Failure analysis and fatigue performance evaluation of a failed connecting rod of reciprocating air compressor. *Engineering Failure Analysis*, ***56***, pp.142-149.

[8] Ali, H.M.M. and Haneef, M., 2015. Analysis of fatigue stresses on connecting rod subjected to concentrated loads at the big end. *Materials today: proceedings*, ***2*****(4-5)**, pp.2094-2103.

[9] Rezvani, M.A., Javanmardi, D. and Mostaghim, P., 2018. Diagnosis of EMD645 diesel engine connection rod failure through modal testing and finite element modeling. *Engineering Failure Analysis*, *92*, pp.50-60.

[10] Abad, M.R.A.A., Ranjbarkohan, M. and Dardashti, B.N., 2011. Dynamic load analysis and optimization of connecting rod of samand engine. *Australian Journal of Basic and Applied Sciences*, ***5*****(12)**, pp.1830-1838.

[11] Lee, M.K., Lee, H., Lee, T.S. and Jang, H., 2010. Buckling sensitivity of a connecting rod to the shank sectional area reduction. *Materials & Design*, ***31*****(6)**, pp.2796-2803.

[12] Kreculj, D. and Rasuo, B., 2018. Impact damage modeling in laminated composite aircraft structures. In *Sustainable Composites for Aerospace Applications* (pp. 125-153). Woodhead Publishing.

[13] Pani, A.R., Patel, R.K. and Ghosh, G.K., 2020. Buckling analysis and material selection of connecting rod to avoid hydro-lock failure. *Materials Today: Proceedings*, ***27***, pp.2121-2126.

[14] Sharma, P.K. and Borse Rajendra, R., 2012. Ftigue analysis and optimisation of connecting rod using finite element analysis. *International Journal of advance research in Science and Engineering*, ***1*****(1)**, pp.3367-337.

[15] Pathade, V.C., Patle, B. and Ingale, A.N., 2012. Stress analysis of IC engine connecting rod by FEM. *International Journal of Engineering and Innovative Technology*, ***1*****(3)**, pp.12-15.

[16] Bansal, R., 2013. Dynamic simulation of connecting rod made of aluminium alloy using finite element analysis approach. *IOSR Journal of Mechanical and Civil Engineering*, ***5*****(2)**, pp.01-05.

[17] Ahmed, G.S., Khany, S.E. and Shareef, S.H., 2014. Design, Fabrication and Analysis of a Connecting rod with Aluminum alloys and carbon fiber. *International Journal of Innovative*

Research in Science, Engineering and Technology, ***3*****(10)**, pp.16674-16687.

[18] Bin, Z., Lixia, J. and Yongqi, L., 2010, January. Finite element analysis and structural improvement of diesel engine connecting rod. In *2010 Second International Conference on Computer Modeling and Simulation* (**Vol. 1**, pp. 175-178). IEEE.

[19] AbhinavGautam, K. and Ajit, P., 2013. Static stress analysis of connecting rod using finite element approach. *IOSR Journal of Mechanical and Civil Engineering (IOSR-JMCE)*, *10*(1), pp.47-51.

[20] He, B.Y., Sun, J.B., Chen, S.Z. and Nie, R., 2013. Crack analysis on the toothed mating surfaces of a diesel engine connecting rod. *Engineering Failure Analysis*, ***34***, pp.443-450.

[21] Londhe, A., Yadav, V. and Sen, A., 2009. *Finite element analysis of connecting rod and correlation with test* (No. 2009-01-0816). SAE Technical Paper.

[22] Rabb, R., 1996. Fatigue failure of a connecting rod. *Engineering Failure Analysis*, ***3*****(1)**, pp.13-28.

[23] Rakic, S., Bugaric, U., Radisavljevic, I. and Bulatovic, Z., 2017. Failure analysis of a special vehicle engine connecting rod. *Engineering failure analysis*, ***79***, pp.98-109.

[24] Witek, L. and Zelek, P., 2019. Stress and failure analysis of the connecting rod of diesel engine. *Engineering Failure Analysis*, ***97***, pp.374-382.

[25] Seralathan, S., Mitnala, S.V., Reddy, R.S.K., Venkat, I.G., Reddy, D.R.T., Hariram, V. and Premkumar, T.M., 2020. Stress analysis of the connecting rod of compression ignition engine. *Materials Today: Proceedings*.

[26] Gaikwad, S.S. and Aitavade, E.N., 2013. Static Analysis Of A Roller Of Gravity Roller Conveyor For Structural Strength & Weight Optimization. *PG student, Prof, Mechanical Engineering Department, Tatyasaheb Kore Institute of Engineering andTechnology, Warananagar, Tal.-Panhala, Dist. Kolhapur-416113, India, International Journal of Advanced Engineering Technology*, *4*.

[27] Muhammad, A., Ali, M.A. and Shanono, I.H., 2020. Design optimization of a diesel connecting rod. *Materials Today: Proceedings*, ***22***, pp.1600-1609.

[28] Lotfy, M.N., Khalifa, Y.A., Dessouki, A.K. and Fathallah, E., 2020. Dynamic Behavior of Steel and Composite Ferry Subjected to Transverse Eccentric Moving Load Using Finite Element Analysis. *Applied Sciences*, ***10*****(15)**, p.5367.

[29] Helal, M.M. and Elsayed, F., 2015. Dynamic behavior of stiffened plates under underwater shock loading. *Materials Testing*, ***57*****(6)**, pp.506-517.

[30] Helal, M. and Fathallah, E., 2020. Finite element analysis and design optimization of a non-circular sandwich composite deep submarine pressure hull. *Materials Testing*, ***62*****(10)**, pp.1025-1032.

[31] Helal, M., Huang, H., Wang, D. and Fathallah, E., 2019. Numerical Analysis of Sandwich Composite Deep Submarine Pressure Hull Considering Failure Criteria. *Journal of Marine Science and Engineering*, *7*(10), p.377.

[32] Fathallah, E., Qi, H., Tong, L. and Helal, M., 2015. Design optimization of lay-up and composite material system to achieve minimum buoyancy factor for composite elliptical submersible pressure hull. *Composite Structures*, ***121***, pp.16-26.

[33] Fathallah, E., Qi, H., Tong, L. and Helal, M., 2015. Numerical investigation of the dynamic response of optimized composite elliptical submersible pressure hull subjected to non-contact underwater explosion. *Composite Structures*, ***121*****,** pp.121-133.

[34] Chen, X. and Liu, Y., 2018. *Finite element modeling and simulation with ANSYS Workbench*. CRC press.

[35] Alkalla, M.G., Helal, M. and Fouly, A., 2021. Revolutionary superposition layout method for topology optimization of nonconcurrent multiload models: Connecting-rod case study. *International Journal for Numerical Methods in Engineering*, ***122*****(5)**, pp.1378-1400.

[36] Arora, J.S., 2017 Chapter 1 - Introduction to Design Optimization, in Introduction to Optimum Design (Fourth Edition), J.S. Arora, Editor, Academic Press: Boston. p. 3-18.